Engineering Science and Technology, an International Journal 22 (2019) 1013–1026

HOSTED BY

Contents lists available at ScienceDirect

Engineering Science and Technology, an International Journal

journal homepage: www.elsevier.com/locate/jestch

Full Length Article

Investigation on SVM-Backstepping sensorless control of five-phase open-end winding induction motor based on model reference adaptive system and parameter estimation

Khadar Saad [a], Kouzou Abdellah [a,*], Hafaifa Ahmed [a], Atif Iqbal [b]

[a] Laboratory of Applied Automation and Industrial Diagnosis, Faculty of Sciences and Technology, B.P 3113, Ziane Achour University, 17000 Djelfa, Algeria
[b] Department of Electrical Engineering, Qatar University at Doha, Qatar

ARTICLE INFO

Article history:
Received 30 July 2018
Revised 25 January 2019
Accepted 25 February 2019
Available online 7 March 2019

Keywords:
Five-phase induction machine
Backstepping control
Sensorless control
Parameters estimation
MRAS technique
Open-end stator winding
SVPWM strategy

ABSTRACT

This paper deals with a new control technique applied to five-phase induction motor under open-end stator winding (FPIM-OESW) topology using the backstepping nonlinear control. The main objective is to improve the dynamics of this kind of machine, which is intended to be used in high power industrial application, where the maintenance is difficult and the fault tolerant is needed to ensure the continuous motor operating mode with minimized number of interruption. This control technique is combined with the Space Vector Pulse Width Modulation (SVPWM) to maintain a fixed switching frequency. In addition, the Model Reference Adaptive System (MRAS) concept is used for the estimation of the load torque, the rotor flux and the rotor speed to overcome the main drawbacks presented with the previous sensorless systems concepts. However, the great sensitivity to the changes of the motor internal parameters and it operating instability problems, especially in low-speed operating region, that causes an estimation error of the rotor speed, is the most disadvantage of the MRAS technique. Therefore, to solve this problem, an estimation method of the motor internal parameters such as the rotor resistance, the stator resistance and the magnetizing inductance, is proposed in this paper. Where, the main aim is to improve furthermore the control performance, to reduce the computational complexity and to minimize the rotor speed estimation error. The obtained simulation results confirm the enhanced performance and the clear efficacy of the proposed control technique under a variety of cases of different operating conditions.

1. Introduction

During the recent years, multi-phase AC machine drives have gained an increasing interest, due to the numerous significant features that they offer when compared to their three-phase machine counterparts, such as increased robustness, reduced torque ripple, reduced stator current per phase, higher torque density and fault tolerance capability [1–3]. Therefore, multi-phase motor drives appear to be an outstanding competitor, especially in industrial application where high power levels are required such as railway traction, naval and aircraft propulsion and aerospace application [4–6]. On the other hand, multilevel inverters have been used widely due their high power capability, especially under high voltage and/or high current industrial application. Indeed, these inverters present several advantages such as reduced dv/dt, lower total harmonic distortion and reduced common-mode voltage [7]. In this context, it has been shown recently that combining these two concepts, especially in high power industrial application can lead to additional benefits. Thus, the work presented in this paper aims to benefit from the merits of the both aforementioned concepts, where a topology based on the opening of the FPIM stator winding neutral point, which is known as "open-end stator winding (OESW)" and supplying the both obtained winding ends by a two basic five-phase two-level inverters, is investigated. This configuration offers some additional benefits over the conventional single-side supplied configurations. It is obvious that if the OESW topology is used, the waveform of the supplied voltage to the FPIM-OESW will present exactly the difference between the two dual inverters output voltages, which is similar to the supplied voltages by one conventional three-level inverter feeding a FPIM under stator star connection.

On the other side, many control techniques have been used, as an example the two well-known control techniques of the

* Corresponding author.
E-mail addresses: s.khadar@univ-djelfa.dz (K. Saad), kouzouabdellah@ieee.org (K. Abdellah), a.hafaifa@univ-djelfa.dz (H. Ahmed), atif.iqbal@qu.edu.qa (A. Iqbal).
Peer review under responsibility of Karabuk University.

https://doi.org/10.1016/j.jestch.2019.02.008
2215-0986/

Nomenclature

Acronyms

MRAS	model reference adaptive system
SVPWM	space vector PWM
FPIM	five phase induction motor
OESW	open-end stator winding
FPIM-OEW	five phase induction motor open-end stator winding

Symbols

$\alpha-\beta-z_1-z_2$	stationary frames
$d-q-x-y$	synchronous frames
i_{sd}, i_{sq}:	$d-q$ frame stator current (in ampere (A))
V_{sd},V_{sq}:	$d-q$ frame stator voltage (in volte (V))
i_{sx}, i_{sy}	stator currents in $x-y$ frame (in ampere (A))
V_{sx},V_{sy}	stator voltage in $x-y$ frame (in volte (V))
ψ_{rd},ψ_{rq}	$d-q$ frame rotor flux (in weber (Wb))
ψ_r	rotor flux (in weber (Wb))
ψ_{sd},ψ_{sq}	stator flux following $d-q$ axis (in weber (Wb))
ψ_s	stator flux (in weber (Wb))
R_s	stator resistance (in ohms (Ω))
L_s	stator inductance (in henry (H))
R_r	rotor resistance (in ohms (Ω))
L_r	rotor inductance (in henry (H))
L_{ls}	leakage inductance of stator (in henry (H))
L_{lr}	leakage inductance of the rotor (in henry (H))
L_m	magnetization Inductance(in henry (H))
T_r	rotor time constants (in seconds (s))
σ	dispersion coefficient (of Blondel)
n_P	pole pairs number
ω	rotor angular speed (in radian per second (Rad/s))
ω_s	synchronous angular speed (in radian per second (Rad/s))
ω_{sl}	slip angular speed (in radian per second (Rad/s))
J	moment of inertia of load and the motor (in Kilogram per meter square (Kg/m^2))
F	viscous friction coefficient (in Newton meter second ($N.m.s$))

field-oriented control [7] and the direct torque control [8], due to their easy implementation. Nevertheless, the major drawbacks of these techniques are their remarkable sensitivity to the changes of the motor parameters and the presence of the torque ripples. To overcome such drawbacks, the backstepping technique based on SVPWM is proposed in this paper. This application, which combines the presented control technique and the proposed motor topology, presents an original work that has not been treated before by other researchers. This control technique offers excellent performance and a better speed tracking response to the reference. Furthermore, it possesses some key advantages such as the inherent robustness to the eventual variations of the motor parameters, which helps improving the dynamic behavior of the motor, the reduction of the torque ripples, the enhancement of the response dynamics, the constant switching frequency due to the use of the SVPWM strategy and the decoupling between their dynamics [9,10].

In the recent year, a number of researchers have proposed several methods to ensure an accurate estimation of the main influencing variables such as the rotor speed and the rotor flux to fulfill the requirement of the sensorless control approach. In this context, to ensure the sensorless control of the three-phase motor, the speed has been estimated by various techniques, the famous one is the extended Kalman filter method [11]. However, because of the sensitivity of such control techniques to the changes in the machine parameters and due to the lack of effective tuning criteria, the estimation becomes inaccurate. The authors in [12] have proposed some methods to estimate the motor speed based on high frequency signal injection. However, they have been obliged firstly to design a system for ensuring the signal injection, which has rendered these techniques to be unsuitable for robust control and furthermore difficult to be implemented practically. An Adaptive Luenberger observer has been designed to ensure the systems states estimation based on the machine model [13]. However, the problem of sensitivity to the changes in the machine parameters (especially the resistances) has made the estimation to be an inaccurate. A full-order sliding mode observer has been proposed where better performance has been obtained, but still some problems have not been solved, such as the influence of the noise characteristic, which affects the precision [14]. Whereas, the chattering problem which has been eliminated using higher order sliding modes, has led to system complexity and has increased the overall computational cost. The Model Reference Adaptive Systems (MRAS) has been firstly introduced in [15], which has become the most used approach in ensuring an accurate estimation of the motor rotor speed and rotor flux, due to its design simplicity, accuracy, fast convergence, reduced computational cost and ease implementation [16,17]. However, it is sensitive to the changes of the motor parameters because the effectiveness of the MRAS is depending strictly on the rotor resistance. It is important to clarify that a small deviation of the estimated rotor flux from the measured rotor flux obtained in real time, leads to an important error in the estimation of the speed. Furthermore, it can be a main cause of instability of the control technique itself. This deviation is due principally to the change of the rotor resistance caused by the increase of the motor internal temperature, which may vary up to 100% of its initial value [18,19]. Consequently, several researchers have proposed many online algorithms for ensuring the accurate estimation of the actual motor rotor resistance. The authors in [20] have used an approach for the estimation of the rotor resistance, which is deduced from the well-known Extended Kalman Filter, where the performance and the power efficiency are significantly improved. In [21], the authors have proposed the fuzzy rotor resistance estimator. However, the obtained results show that it does not guarantee a good estimation of the motor rotor resistance when the reference speed changes suddenly. The work presented in [22], shows that the estimation error of the motor rotor resistance converges to 10% using Luenberger observer, but this error weakens the performance of the control system. In [23], the authors have presented a rotor resistance estimator based on the reactive-power reference model, but the main drawback of this estimation is its very sensitivity to the load variation. On the other side, it was found that the stator resistance is not dominant in the high speed range, so a possible estimation error will not affect the rotor flux calculations. Contrarily, in low-speed operation, the precise estimation of the stator resistance value becomes critical [24]. Many researchers have orientated their works on the estimation of the stator resistance, where a method using a full-order flux observer has been proposed to ensure an improved sensorless control [25]. In [26], the reactive power has been evaluated first, then the stator and rotor flux have been calculated next, where an expression has been derived finally for the stator resistance calculation based on the previously calculated quantities. On the other side, the error quantity in the observer-based systems proposed in [27,28], has served as an input into the stator resistance adaptation mechanism which has been determined based

on the difference between the measured and the observed stator currents, where the proportional integral (PI) controllers have been used for this purpose. But it may be noted that the problems with this methods are the response time and the error estimation, especially in the presence of sudden changes in the speed or load torque. These methods also require more computing time due to the complexity of solving differential equations. In the same context, it has been found that the mismatch of magnetizing inductance affects the accuracy of the estimated rotor speed, especially when the speed variation is required within a wide operation range. It is well known that the magnetizing inductance is depending strongly on the motor magnetizing characteristic, which means that any eventual change in the magnetizing inductance is followed by the machine magnetizing flux change [29]. Furthermore, in the field-weakening region, it is required to reduce the rotor flux reference as the rotor speed increases over its nominal value. The drawback of this region is that the variation of the magnetizing inductance in the machine affects the motor operation. It is therefore necessary to provide an online estimation of the magnetizing inductance. Indeed, some online estimation approaches have been proposed for improving the motor operation in [29,30]. In [31] the difference between the observed rotor flux and the reference model are used to estimate the magnetizing inductance, but in electrical vehicle (EV) applications, the operating speed range is wide and the speed changes frequently, which limits the accuracy of the compensation method. Based on the presented state of the art in this introduction, it can be concluded that without the motor parameters estimation, the desired performances response of the motor control cannot be obtained [23], the system control stability cannot be ensured and the motor dynamic behavior can be degraded drastically [10], especially in the presence of the variations of the load torque and the speed.

The main contributions of the proposed control scheme proposed in this paper are to solve or reduce the aforementioned disadvantages. They are summarized as follows:

- The design of a simple control scheme that combines some previous control techniques to be applied for the sensorless control of FPIM-OESW topology. Where, the investigation on the proposed control and the proposed motor topology presented in this paper, is an original work that has not been treated before by the researchers.
- The guarantee of an accurate estimation of motor parameters, especially the stator resistance, the rotor resistance and the magnetizing inductance where the main aim is to minimize the error and the computational time in comparison with the previous works [21–23,27,28,31,32].
- The improvement of the proposed control robustness based on the estimation of the applied load torque on the motor. Where, the proposed method proposed in this paper is based on a simple algorithm compared to the works presented in [33,34].

The present paper is structures as follows: In Section II, a brief review of the dual two-level inverter feeding the studied FPIM-OESW is presented. Then, a review on the principle of the used backstepping control based on SVPWM algorithm is explained. In section III, the stability of the proposed control technique based on Lyapunov theory is discussed. Section IV presents the investigation and discussion of the use of the MRAS-based estimation in ensuring the accurate estimation of the motor rotor speed, the rotor flux and the load torque. The design processes proposed in this paper to estimate the motor parameters (magnetizing inductance, rotor and stator resistance) are presented in details in Section V. The obtained simulation results are discussed in section VI. Finally, the present paper ends with a general conclusion.

2. The five-phase induction motor open-end stator winding (FPIM-OESW)

2.1. The FPIM modeling

The FPIM model has been formulated previously based on the commonly used simplifying assumptions [7,35]. Where this model has been presented in the synchronous reference following the $(d-q-x-y)$ axis and in the stationary reference following the $(\alpha-\beta-z_1-z_2)$ axis [36,37]. In the synchronous reference, two orthogonal frames called $d-q$ and $x-y$ are used. Where, the components $d-q$ are responsible for developing the fluxes and the torque, while the remaining $x-y$ components generate the machine losses. Taking into account the orientation following the rotor flux, which means $\psi_{rd}=\psi_r$ and $\psi_{rq}=0$ [7,10,18,38], the dynamic equation of the FPIM in the $d-q-x-y$ reference frame can be presented as follows [38]:

$$\begin{cases} \frac{di_{sd}}{dt}=\alpha_1 i_{sd}+\omega i_{sq}+\alpha_2\psi_r+\frac{1}{\sigma L_s}V_{sd} \\ \frac{di_{sq}}{dt}=\alpha_1 i_{sq}-\omega i_{sd}+\alpha_2\psi_r+\frac{1}{\sigma L_s}V_{sq} \\ \frac{di_{sx}}{dt}=-\frac{R_s}{L_{ls}}i_{sx}+\frac{1}{L_{ls}}V_{sx} \\ \frac{di_{sy}}{dt}=-\frac{R_s}{L_{ls}}i_{sy}+\frac{1}{L_{ls}}V_{sy} \end{cases} \quad (1)$$

$$\begin{cases} \frac{d\psi_{rd}}{dt}=\frac{d\psi_r}{dt}=\frac{L_m}{T_r}i_{sd}-\frac{\psi_r}{T_r} \\ \frac{d\psi_{rq}}{dt}=0=\frac{L_m}{T_r}i_{sq}-\omega_{sl}\psi_r \\ \frac{d\omega}{dt}=\alpha_3\psi_r i_{sq}-\frac{n_p}{J}T_L-\frac{F}{J}\omega \end{cases} \quad (2)$$

where, r and s subscripts refer to the rotor and the stator respectively.

With: $\alpha_1=\frac{L_m^2 R_r+R_s L_r^2}{\sigma L_s L_r^2}$, $\alpha_2=\frac{L_m R_r}{\sigma L_s L_r}$, $\alpha_3=\frac{n_p^2 L_m}{J L_r}$, $\sigma-1-\frac{L_m}{L_s L_r}$, $\omega=\omega_s-\omega_{sl}$.

From Eqs. (1) and (2), the electrical model equivalent schema of FPIM on a synchronously reference frame can be obtained as shown in Fig. 1 [39,40]. This model contains two decoupled equivalent circuit following the two axis of $d-q$ frame, which is similar to the three-phase model, two decoupled equivalent circuit following the two axis of x-y model, and two decoupled equivalent circuit for the rotor following the two axis of x-y model which have simple resistive inductive representative equivalent circuit.

2.2. The dual inverter supplying a FPIM-OESW

Fig. 2, shows the principle circuit of the studied topology presented in this paper [7,8], where only one DC source is used to provide the required input power to the dual two-level inverter feeding the FPIM-OESW. The two inverters constituting the dual two-level inverter are marked by indices 1 and 2 as shown in Fig. 2. On the other side, the motor stator windings of the five phases are equally displaced by an angle $\theta=2\pi/5$, where these stator windings are supplied from the both sides by the two inverters. By using this topology, the common mode voltage is forced to zero due to the connection path between the two inverters [41]. Furthermore, more protection can be ensured for the bearing, where its lifespan can be increased, this is due to the absence of the circulating current through the motor case that was initially created by the common mode voltage in the conventional topology.

Taking into account that the two inverters output terminals are connected to the motor terminals of the corresponding phases. Thus, the phase voltages across each stator winding can be obtained by applying Kirchhoff's law to Fig. 2 as follows [7]:

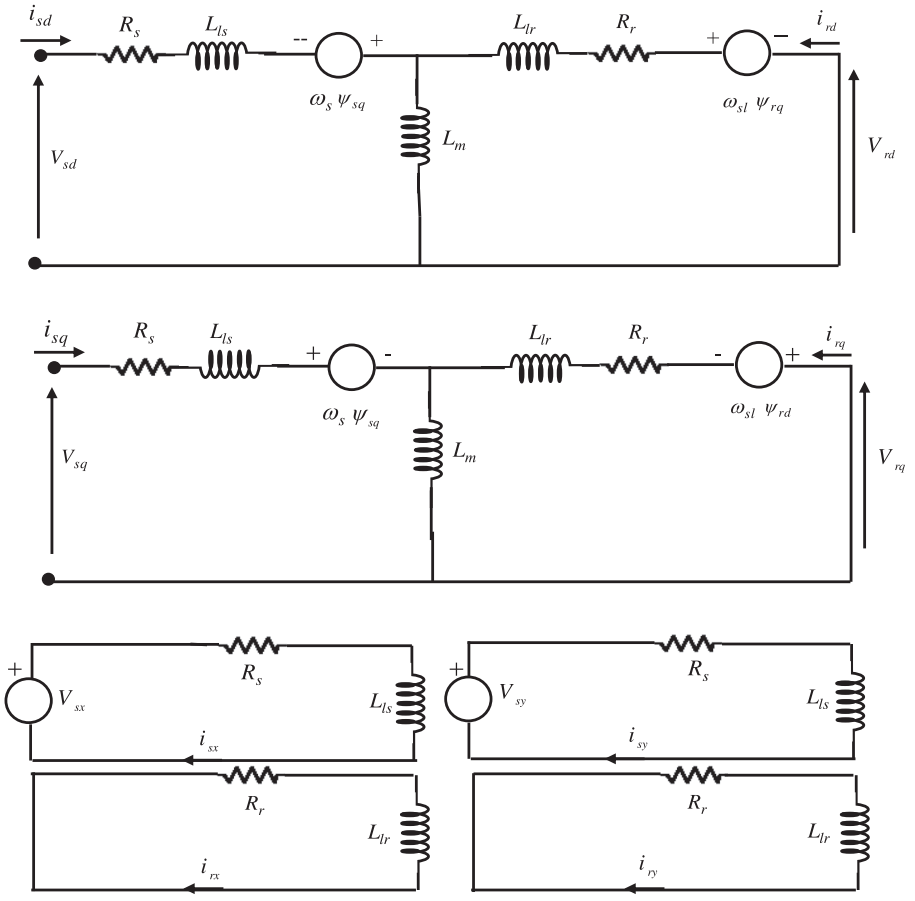

Fig. 1. A d-q-x-y axis equivalent circuit of the five phase Induction machine in an arbitrary synchronously rotating.

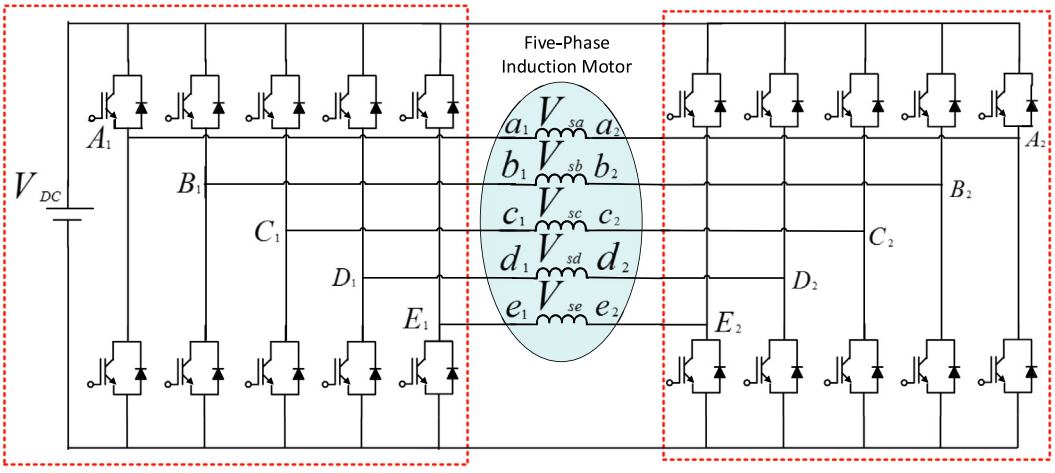

Fig. 2. The principle topology of a dual-inverters connected to FPIM-OESW with one DC source.

$$\begin{cases} V_{sa} = V_{A1} - V_{A2} \\ V_{sb} = V_{B1} - V_{B2} \\ V_{sc} = V_{C1} - V_{C2} \\ V_{sd} = V_{D1} - V_{D2} \\ V_{se} = V_{E1} - V_{E2} \end{cases} \tag{3}$$

where: (V_{A1},V_{B1}, V_{C1}, V_{D1}, V_{E1}) and (V_{A2},V_{B2}, V_{C2}, V_{D2}, V_{E2}) are the five-phase output voltages of the first inverter and the second inverter respectively. The output voltage of the two inverters in the two stationary frames $\alpha - \beta$ and $z_1 - z_2$ are obtained based on the five-phase output voltages of each inverter $i = \{1\ ,\ 2\}$ as follows:

$$\begin{cases} V_{\alpha\beta i} = 2/5(V_{Ai} + aV_{Bi} + a^2 u_{Ci} + a^3 V_{Di} + a^4 V_{Ei}) \\ V_{z_1 z_2 i} = 2/5(V_{Ai} + a^2 V_{Bi} + a^4 V_{Ci} + a^6 V_{Di} + a^8 V_{Ei}) \end{cases} \tag{4}$$

where: $a = e^{(j2\pi/5)}$.

Using Eqs. (3) and (4), Eq. (5) is obtained:

$$\begin{cases} V_{s\alpha\beta} = V_{\alpha\beta 1} - V_{\alpha\beta 2} \\ V_{sz_1z_2} = V_{sz_1z_2 1} - V_{sz_1z_2 2} \end{cases} \quad (5)$$

The space vector representing the different possibilities of the output voltage and their eventual switching states of the used five-phase inverter in the $\alpha - \beta$ frame and $z_1 - z_2$ frame are shown in Fig. 3a and b respectively. It is obvious that in the $\alpha - \beta$ frame, there are thirty none zero space vectors and two zero space vectors which are corresponding to all the eventual states of the switches of the two-level five phase inverter as shown in Fig. 3a. The same number of none zero vectors and zero vectors, following the same states of the switches are obtained in the $z_1 - z_2$ frame as shown in Fig. 3b.

The thirty non-zero space voltage vectors presenting the active vectors can be defined following three main groups of ten large vectors, ten medium vectors and ten small vectors. On the other side, the plane of the $\alpha - \beta$ frame and $z_1 - z_2$ frame are divided into ten similar sectors, where each sector covers an angle of $\pi/5$ degree as shown in Fig. 3. The voltage space vectors in $z_1 - z_2$ frame do not contribute in the production of the developed torque by the motor, but they can contribute in increasing the power losses in the stator windings [7].

3. The principle of the proposed control

3.1. Backstepping control

The main idea behind the backstepping control technique is to ensure the stability of the nonlinear studied system [42]. Indeed, it is based on the decomposition of the entire control system to subsystems, where for each subsystem, a virtual control law is calculated, which serves as a reference for the following subsystem in obtaining the accurate control law of the whole studied system. In the present study, the designed control law has to ensure the pursuit of the reference rotor speed ω^* and at the same time to keep the reference rotor flux ψ_r^* constant. In this paper, at each stage a virtual control is generated to ensure the convergence of the system to its equilibrium state based on the Lyapunov function that is used with the proposed backstepping controller. Indeed, it has been found in the present study that the only problem faced when using the backstepping controller is the building of the Lyapunov function adapted to the studied system. However, as the appropriate Lyapunov function is constructed, the asymptotic stability of the system will be ensured. However, there is no exact theoretical basic for finding the appropriate Lyapunov function of the specified system, but in all most control cases it is based essentially on the experience and the intuition of the control designer. This can be a considered the main major drawback of using the Lyapunov function with the proposed controller, But this disadvantage can be omitted totally when the function is well defined [13,38,42–44]. Indeed, Lyapunov function is a very powerful tool for testing and finding sufficient stability of dynamical system conditions. The stability depends only on the variations (sign of the derivative), or a function which is equivalent, along the trajectory of the system. Furthermore, an important merit of Lyapunov function-based stability analysis in backstepping control is that the actual numerical solution of the differential equations is not required and it can be used for arbitrary differential equations [45].

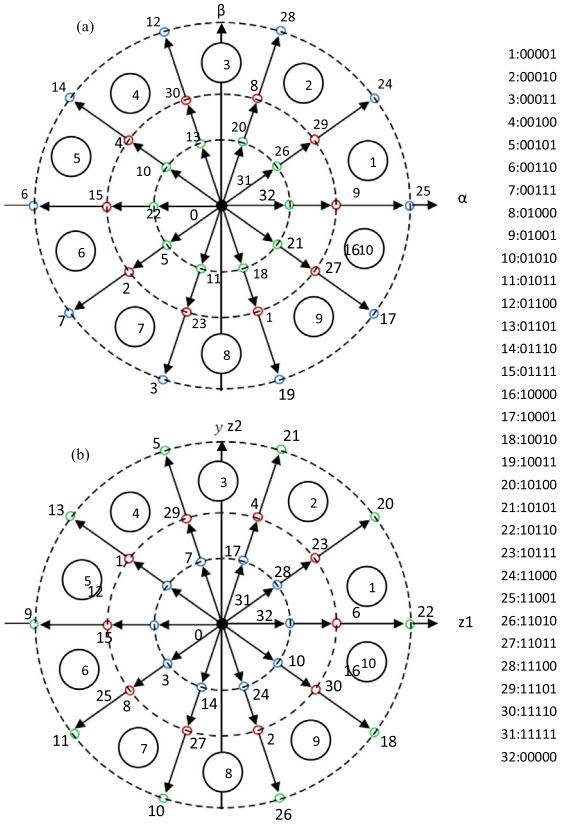

Fig. 3. The voltage space vectors and the switching states of the five-phase inverter 1 in: (a) $\alpha - \beta$ frame and (b) $z_1 - z_2$ frame.

The first step consists in defining the errors and the dynamics of the variables to be controlled such as the rotor speed ω and the rotor flux ψ_r, where the dynamics of the variables is presented by their corresponding derivatives. In the present paper, these errors are corresponding to the error between the real rotor speed and the reference rotor speed (e_ω) and the error between the real rotor flux and the reference rotor flux (e_ψ) respectively, which are expressed as follows [10,13]:

$$\begin{cases} e_\omega = \omega^* - \omega \\ e_\psi = \psi_r^* - \psi_r \\ \dot{e}_\omega = \dot{\omega}^* - \dot{\omega} \\ \dot{e}_\psi = \dot{\psi}_r^* - \dot{\psi}_r \end{cases} \quad (6)$$

By replacing $\dot{\omega} = d\omega/dt$ and $\dot{\psi}_r = d\psi/dt$ with their expressions presented in Eq. (2), Eq. (6) becomes:

$$\begin{cases} \dot{e}_\omega = \dot{\omega}^* - \alpha_3 \psi_r i_{sq} + \frac{n_p}{J} T_L + \frac{F}{J}\omega \\ \dot{e}_{\psi_r} = \dot{\psi}_r^* + \frac{\psi_r}{T_r} - \frac{L_m}{T_r} i_{sd} \end{cases} \quad (7)$$

The main aim of the required control is to ensure the stability of the real rotor speed and the rotor flux control loops. Where, the virtual inputs presenting the references stator currents i_{sd}^* and i_{sq}^* are used to fulfill this requirement and which can be obtained using the Lyapunov functions control. The first chosen Lyapunov function V_1 that is associated with e_ω and e_ψ is defined as follows [10]:

$$V_1 = \frac{1}{2}\left(e_\omega^2 + e_\psi^2\right) \quad (8)$$

Therefore, its derivative can be written as:

$$\dot{V}_1 = \dot{e}_\omega \cdot e_\omega + \dot{e}_\psi \cdot e_\psi \quad (9)$$

Using Eq. (7), Eq. (9) becomes:

$$\dot{V}_1 = e_\omega\left(\dot{\omega}^* - \alpha_3 \psi_r i_{sq} + \frac{n_p}{J} T_L + \frac{F}{J}\omega\right) + e_\psi\left(\dot{\psi}_r^* + \frac{\psi_r}{T_r} - \frac{L_m}{T_r} i_{sd}\right) \quad (10)$$

To fit the requirement of the Lyapunov stability conditions, Eq. (10) can be reformulated as follows:

$$\dot{V}_1 = -K_\omega \cdot e_\omega^2 - K_\psi \cdot e_\psi^2 + e_\omega\left(K_\omega \cdot e_\omega + \dot{\omega}^* - \alpha_3 \psi_r\, i_{sq} + \frac{n_p}{J} T_L + \frac{F}{J}\omega\right) + e_\psi\left(K_\psi \cdot e_\psi + \dot{\psi}_r^* + \frac{\psi_r}{T_r} - \frac{L_m}{T_r} i_{sd}\right) \tag{11}$$

To achieve the asymptotic stability of the both control loops, the Lyapunov condition $\dot{V}_1 \prec 0$ has to be satisfied, which means that the following condition have to be met:

$$\begin{cases} K_\omega \cdot e_\omega + \dot{\omega}^* - \alpha_3 \psi_r\, i_{sq} + \frac{n_p}{J} T_L + \frac{F}{J}\omega = 0 \\ K_\psi \cdot e_\psi + \dot{\psi}_r^* + \frac{\psi_r}{T_r} - \frac{L_m}{T_r} i_{sd} = 0 \\ K_\omega \succ 0 \\ K_\psi \succ 0 \end{cases} \tag{12}$$

This yields to the final form of the Lyapunov function derivative:

$$\dot{V}_1 = -K_\omega \cdot e_\omega^2 - K_\psi \cdot e_\psi^2 \tag{13}$$

Based on Eq. (12), the virtual control inputs presenting the stator reference currents i_{sd}^* and i_{sq}^*, which allow generating the stabilizing functions using the stability condition of Lyapunov theory, can be obtained as follows:

$$\begin{cases} i_{sd}^* = \frac{T_r}{L_m}\left(K_\psi \cdot e_\psi + \dot{\psi}^* + \frac{\psi_r}{T_r}\right) \\ i_{sd}^* = \frac{1}{\alpha_3 \psi_r}\left(K_\omega \cdot e_\omega + \dot{\omega}^* + \frac{F\omega}{J} + \frac{T_L n_p}{J}\right) \end{cases} \tag{14}$$

This reference current will be used in the following step for constructing the control law. Indeed, in the second step, the control law V_{sd}, V_{sq}, V_{sx} and V_{sy} of the whole system are determined, where the two new errors of the current stator components along $d-q$ axis and $x-y$ axis are defined as follows [44]:

$$\begin{cases} e_{i_{sd}} = i_{sd}^* - i_{sd} \\ e_{i_{sq}} = i_{sq}^* - i_{sq} \\ e_{i_{sx}} = i_{sx}^* - i_{sx} \\ e_{i_{sy}} = i_{sy}^* - i_{sy} \end{cases} \tag{15}$$

Furthermore, their dynamics are expressed as:

$$\begin{cases} \dot{e}_{i_{sd}} = \dot{i}_{sd}^* - \dot{i}_{sd} \\ \dot{e}_{i_{sq}} = \dot{i}_{sq}^* - \dot{i}_{sq} \\ \dot{e}_{i_{sx}} = \dot{i}_{sx}^* - \dot{i}_{sx} \\ \dot{e}_{i_{sq}} = \dot{i}_{sy}^* - \dot{i}_{sy} \end{cases} \tag{16}$$

Based on the derivative of Eq. (15) and Eq. (1), the derivatives of the stator current errors can be calculated:

$$\begin{cases} \dot{e}_{i_{sd}} = \frac{di_{sd}^*}{dt} - \alpha_1 i_{sd} - \omega\, i_{sq} - \alpha_2 \psi_r - \frac{1}{\sigma L_s} V_{sd} \\ \dot{e}_{i_{sq}} = \frac{di_{sq}^*}{dt} - \alpha_1 i_{sq} + \omega\, i_{sd} - \alpha_2 \psi_r - \frac{1}{\sigma L_s} V_{sq} \\ \dot{e}_{i_{sx}} = \frac{di_{sx}^*}{dt} - \frac{R_s}{L_{ls}} i_{sx} - \frac{1}{L_{ls}} V_{sx} \\ \dot{e}_{i_{sq}} = \frac{di_{sy}^*}{dt} - \frac{R_s}{L_{ls}} i_{sy} - \frac{1}{L_{ls}} V_{sy} \end{cases} \tag{17}$$

For the stability study, the new Lyapunov function V_2 is defined taking into account the three errors such as the rotor speed error, the rotor flux error and the stator currents error, which is expressed as follows:

$$V_2 = \frac{1}{2}\left(e_\psi^2 + e_\omega^2 + e_{i_{sd}}^2 + e_{i_{sq}}^2 + e_{i_{sx}}^2 + e_{i_{sy}}^2\right) \tag{18}$$

Hence, the derivative of V_2 is obtained:

$$\dot{V}_2 = \left(e_\psi \dot{e}_\psi + e_\omega \dot{e}_\omega + e_{i_{sd}} \dot{e}_{i_{sd}} + e_{i_{sq}} \dot{e}_{i_{sq}} + e_{i_{sz1}} \dot{e}_{i_{sz1}} + e_{i_{sz2}} \dot{e}_{i_{sz2}}\right) \tag{19}$$

By substituting Eq. (17) into Eq. (19), while keeping the first parameters K_ω and K_ψ the same as the ones used in Eq. (13), the derivative of V_2 can be rewritten as follows:

$$\dot{V}_2 = A_1 + A_2 + A_3 + A_4 + A_5 \tag{20}$$

With:

$$\begin{cases} A_1 = \left(-K_\omega e_\omega^2 - K_\psi e_\psi^2 - K_{i_{sd}} e_{i_{sd}}^2 - K_{i_{sq}} e_{i_{sq}}^2 - K_{i_{sx}} e_{i_{sx}}^2 - K_{i_{sy}} e_{i_{sy}}^2\right) \\ A_2 = e_{i_{sd}}\left(K_{i_{sd}} e_{i_{sd}} + \frac{di_{sd}^*}{dt} - \alpha_1 i_{sd} - \omega\, i_{sq} - \alpha_2 \psi_r - \frac{1}{\sigma L_s} V_{sd}\right) \\ A_3 = e_{i_{sq}}\left(K_{i_{sq}} e_{i_{sq}} + \frac{di_{sq}^*}{dt} - \alpha_1 i_{sq} + \omega\, i_{sd} - \alpha_2 \psi_r - \frac{1}{\sigma L_s} V_{sq}\right) \\ A_4 = e_{i_{sx}}\left(K_{i_{sx}} e_{i_{sx}} + \frac{di_{sx}^*}{dt} - \frac{R_s}{L_{ls}} i_{sx} - \frac{1}{L_{ls}} V_{sx}\right) \\ A_5 = e_{i_{sy}}\left(K_{i_{sy}} e_{i_{sy}} + \frac{di_{sy}^*}{dt} - \frac{R_s}{L_{ls}} i_{sy} - \frac{1}{L_{ls}} V_{sy}\right) \end{cases}$$

To obtain a negative derivative of the Lyapunov function V_2, the following conditions have to be satisfied:

$$\begin{cases} K_{i_{sd}} e_{i_{sd}} + \frac{di_{sd}^*}{dt} - \alpha_1 i_{sd} - \omega\, i_{sq} - \alpha_2 \psi_r - \frac{1}{\sigma L_s} V_{sd} = 0 \\ K_{i_{sq}} e_{i_{sq}} + \frac{di_{sq}^*}{dt} - \alpha_1 i_{sq} + \omega\, i_{sd} - \alpha_2 \psi_r - \frac{1}{\sigma L_s} V_{sq} = 0 \\ K_{i_{sx}} e_{i_{sx}} + \frac{di_{sx}^*}{dt} - \frac{R_s}{L_{ls}} i_{sx} - \frac{1}{L_{ls}} V_{sx} = 0 \\ K_{i_{sy}} e_{i_{sy}} + \frac{di_{sy}^*}{dt} - \frac{R_s}{L_{ls}} i_{sy} - \frac{1}{L_{ls}} V_{sy} = 0 \\ K_{i_{sd}} \succ 0,\ K_{i_{sd}} \succ 0,\ K_{i_{sd}} \succ 0 \text{ and } K_{i_{sd}} \succ 0 \end{cases} \tag{21}$$

The final step in the design of the control law is based on defining the expressions of the stator voltage references which are given by the following expressions:

$$\begin{cases} V_{sd} = \sigma L_s\left(K_{i_{sd}} e_{i_{sd}} + \frac{di_{sd}^*}{dt} - \alpha_1 i_{sd} - \omega\, i_{sq} - \alpha_2 \psi_r\right) \\ V_{sq} = \sigma L_s\left(K_{i_{sq}} e_{i_{sq}} + \frac{di_{sq}^*}{dt} - \alpha_1 i_{sq} + \omega\, i_{sd} - \alpha_2 \psi_r\right) \\ V_{sx} = L_{ls}\left(K_{i_{sx}} e_{i_{sx}} + \frac{di_{sx}^*}{dt} - \frac{R_s}{L_{ls}} i_{sx}\right) \\ V_{sy} = L_{ls}\left(K_{i_{sy}} e_{i_{sy}} + \frac{di_{sy}^*}{dt} - \frac{R_s}{L_{ls}} i_{sy}\right) \end{cases} \tag{22}$$

The parameters K_ω, K_ψ, $K_{i_{sd}}$, $K_{i_{sq}}$, $K_{i_{sx}}$ and $K_{i_{sy}}$ that have been used in our proposed control are positive and they have been chosen to achieve the improved requirement of the proposed backstepping control such as a faster dynamic of the stator currents, the rotor flux and the rotor speed. Where their accurate values selection will improve the dynamic of the closed loop and hence guarantee the stability of the controlled system [38,44]. Indeed, the values of these parameters used in this paper, have been chosen based on the best values, which have been obtained through several simulation experiences, where the main criterion of selection was to fit the best dynamic requirement of the stator current, the rotor flux and the rotor speed.

At the end of this section, it important to clarify the effect of the "explosion of terms" problem that is inherent in the standard backstepping control and presents its main limitation as it was explained in several previous works. Indeed, this problem can be appeared due to the repeated analytic time derivative of the control input and it inevitably leads to the algorithm complexity, the increase of the computation cost, and the difficulty of the controller design for system with high order. Fortunately, this problem can be solved using a kind of filters such as the first-order filter, the command filters and the robust second order filters to overcome the aforementioned drawbacks and to avoid the problem of "explosion of terms" problem. In the present work, this problem has not been occurred due to the nature of the control inputs, the accu-

rate design of the controller and the good choice of the Lyapunov function. The simulation results obtained in the present paper under different scenarios proves clearly that the proposed controller can overcome this main limitation of the standard backstepping controller.

3.2. The used SVPWM technique

The use of the dual two-level inverters requires a total number of $2^5 \times 2^5$ voltage space vectors, i.e. 1024 possible switching states. However, due to the larger number of possible space vectors it is not evident technically to use all these switching states in the SVPWM [7]. Indeed, many previous works have investigated on the SVM for such kind of inverter and it is actually the subject of several researches [46]. In this paper, a very simple SVPWM scheme, which has been proposed previously in [7] is used, where the number of space vectors is 32 as explained in Fig. 3. In this scheme, the reference voltage is divided equally between the both inverters i.e., each inverter produces the half of the required voltage. The principle of this technique, which is applied to the both modulators SVM_1 and SVM _2 of the both used inverters in the dual topology, is shown in Fig. 4.

According to Fig. 4, the reference voltage space vector lying in the considered sector is synthesized using the appropriate switching times, which are corresponding to the six selected voltage space vectors, two long voltage space vectors, two medium voltage space vectors and two zero voltage vectors which are used in all sectors. The active vectors are selected from the concerned sector. For example, for SVM_1, the reference stator voltage space vector V_{s1} is found in Sector 1 as shown in Fig. 4a, it can be synthesized based on the two long voltage space vectors: V_{25}, V_{24}, and the two medium voltage space vectors: V_{16}, V_{29} and two zero voltage vectors: V_0, V_{31}.

4. The model reference adaptive system (MRAS) technique

4.1. Estimation of the rotor speed and the rotor flux

The model reference adaptive system (MRAS) technique presented in this paper, is the original one proposed in [16,47,48], its basic principal is shown in Fig. 5. Indeed, the main aim of this estimation technique is to provide the estimated rotor speed and the estimated rotor flux under the assumptions that the only available input variables for the measurement are the stator currents and the supplied voltages. It is based on using two models, the first one is the reference model representing the stator voltage model, which is independent of the rotor speed, and the second one is the adjustable model representing the stator current model, which

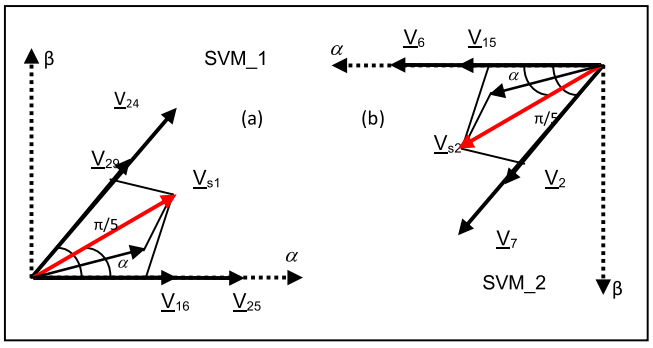

Fig. 4. The principle of determining the active space vectors of the dual-inverter for: a) SVM 1 and b) SVM 2.

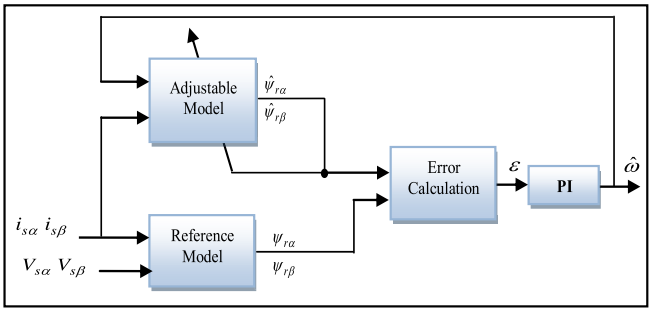

Fig. 5. The block diagram of the speed estimator based on MRAS technique.

uses the rotor speed as a parameter of the motor. The two models are defined in the stationary $\alpha - \beta$ frame as follows [16,47,48]:

- Reference Model:

$$\begin{cases} \frac{d\psi_{r\alpha}}{dt} = \frac{L_r}{L_m}\left(V_{s\alpha} - R_s i_{s\alpha} - \sigma L_s \frac{di_{s\alpha}}{dt}\right) \\ \frac{d\psi_{r\beta}}{dt} = \frac{L_r}{L_m}\left(V_{s\beta} - R_s i_{s\beta} - \sigma L_s \frac{di_{s\beta}}{dt}\right) \end{cases} \quad (23)$$

- Adjustable model

$$\begin{cases} \frac{d\hat{\psi}_{r\alpha}}{dt} = \frac{R_r L_m}{L_r} i_{s\alpha} - \frac{R_r}{L_r}\hat{\psi}_{r\alpha} + \hat{\omega}\cdot\hat{\psi}_{r\alpha} \\ \frac{d\hat{\psi}_{r\beta}}{dt} = \frac{R_r L_m}{L_r} i_{s\beta} - \frac{R_r}{L_r}\hat{\psi}_{r\beta} - \hat{\omega}\cdot\hat{\psi}_{r\beta} \end{cases} \quad (24)$$

The error signals in the $\alpha - \beta$ frame, between the outputs of the two models is given by the following equation:

$$\varepsilon = \hat{\psi}_r \times \psi_r = [\hat{\psi}_{r\alpha}\ \hat{\psi}_{r\beta}] \otimes [\psi_{r\alpha}\ \psi_{r\beta}] = \hat{\psi}_{r\alpha}\cdot\psi_{r\beta} - \hat{\psi}_{r\beta}\cdot\psi_{r\alpha} \quad (25)$$

where "$\otimes$" is the cross product of the two vectors.

The obtained errors signals are used as the inputs of a PI controller that is designed to ensure the MRAS stability. Whereas, the output signal of the PI controller presents the estimated rotor speed used in adjusting the adjustable model until the performance criteria is satisfied. The estimated rotor speed can be expressed as follows:

$$\hat{\omega} = K_p \cdot \left(\hat{\psi}_{r\alpha}\cdot\psi_{r\beta} - \hat{\psi}_{r\beta}\cdot\psi_{r\alpha}\right) + K_i \cdot \int \left(\hat{\psi}_{r\alpha}\cdot\psi_{r\beta} - \hat{\psi}_{r\beta}\cdot\psi_{r\alpha}\right) dt \quad (26)$$

where: $i_{s\alpha}$, $i_{s\beta}$ and $V_{s\alpha}$, $V_{s\beta}$ are the measured stator currents and voltages in the $\alpha - \beta$ frame respectively, K_p and K_i are the proportional and the integral parameters respectively.

4.2. Load torque estimation

The mechanical equation of the studied FPIM is expressed as follows:

$$\frac{d\omega}{dt} = \frac{1}{J}(T_e - T_L) - \frac{F}{J}\omega \quad (27)$$

where, the load torque T_L can be known or it can be measured using a mechanical sensor. In this paper to avoid the use of the torque sensor and to improve the backstepping control performance, a load torque estimator is proposed for the estimation of the applied load torque on the motor. This estimator enables to rebuild the load torque through the record of the rotor flux and the rotor speed, which are estimated based on the MRAS technique. Finally, from (24) and

(27), the load torque estimation can be performed using the following expression:

$$\hat{T}_L = \frac{pL_m}{L_r}\left(\hat{\psi}_{r\alpha} i_{s\beta} - \hat{\psi}_{r\beta} i_{s\alpha}\right) - J\frac{d\hat{\omega}}{dt} - F\hat{\omega} \tag{28}$$

The global scheme of the block diagram of the rotor speed estimation and the load torque estimation based on MRAS model is shown in Fig. 6.

5. Motor parameters estimation

The most important disturbances which can have an important influence on the accuracy of the estimated rotor speed obtained based on the MRAS and which can lead to the system control failure, is the sensitivity to the variation of some parameters of the motor, such as the stator and rotor windings resistances (R_s,R_r) and the magnetizing inductance (L_m). On the other side, the rotor position error is a more serious problem, especially at very low speed, which can lead to the control failure [24]. Therefore, this paper focuses in integrating the motor parameters estimation in the proposed control technique, where the main aim is to overcome the main problem of the variation of motor parameters, which is faced when the estimation is based on MRAS technique.

5.1. Stator resistance estimation

It is well known that the motor stator resistance varies during the motor operation state due mainly to the variation of the stator windings temperature [49]. Therefore, to ensure the on-line estimation of the stator resistance, a simple PI controller is used. The adaptation process is based on the following equation:

$$\varepsilon_{R_s} = i_s\left[\psi_r - \hat{\psi}_r\right]^T = \left[i_{s\alpha}\ i_{s\beta}\right] \cdot \begin{bmatrix} \psi_{r\alpha} - \hat{\psi}_{r\alpha} \\ \psi_{r\beta} - \hat{\psi}_{r\beta} \end{bmatrix} \tag{29}$$

Which yields to:

$$\varepsilon_{R_s} = i_{s\alpha}\left(\psi_{r\alpha} - \hat{\psi}_{r\alpha}\right) + i_{s\beta}\left(\psi_{r\beta} - \hat{\psi}_{r\beta}\right) \tag{30}$$

The stator resistance estimation can be defined based on the adaptation process as follows:

$$\hat{R}_s = R_s + K_{PR_s} \cdot \varepsilon_{R_s} + K_{IR_s} \int \varepsilon_{R_s} \cdot dt \tag{31}$$

Where; K_{PR_s} and K_{IR_s} are the proportional and the integral parameters of the PI controller used in the stator resistance adaptation process respectively.

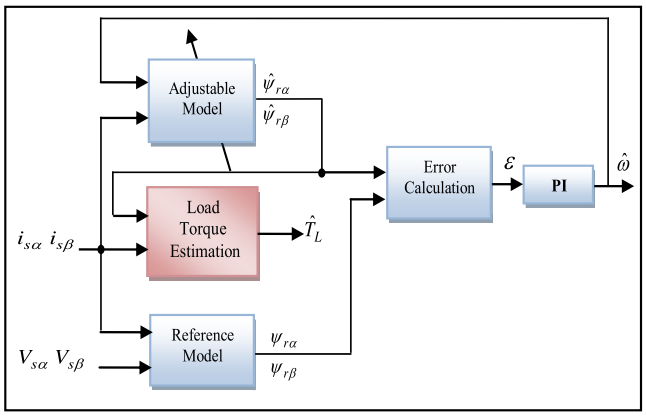

Fig. 6. The block diagram of the speed estimator and Load torque estimator based on MRAS model.

5.2. Rotor resistance estimation

The rotor resistance plays an important task in determining the dynamics behaviors of the induction motor. Therefore, an accurate on-line identification of the rotor resistance value under the actual operating state has an important impact in obtaining a precise on-line estimation of the rotor flux to ensure the control of the motor (see Eq. (24)). In this work, a simple estimation method for the identification of the rotor resistance $\hat{R}_r$ in real time, which is based on the estimated stator resistance $\hat{R}_s$ can be obtained following Eq. (31), where the main aim is to simplify the control and to reduce the used algorithm cost. The rotor-estimated resistance expression, which is developed in this paper is based on the previous proposed method in [50]. Hence, the rotor-estimated resistance can be performed as follows:

$$\hat{R}_r = R_r\left(1 + \frac{\delta_2}{\delta_1}\left(\frac{\hat{R}_s}{R_s} - 1\right)\right) \tag{32}$$

Where; δ_1 and δ_1 are the temperature coefficient at 20 °C of the metals used in the stator and rotor windings respectively. If both winding are made from copper then $\delta_1 = \delta_2 \approx 0.00386$, if the rotor conductor or bars are made from aluminum then $\delta_1 \approx 0.00429$ and $\delta_1 \approx 0.00386$.

5.3. Magnetizing inductance estimation

The magnetizing flux is a function of the stator current and stator flux. Thus the estimated magnetizing flux can be defined in the $\alpha - \beta$ frame as follows:

$$\begin{cases} \hat{\psi}_{m\alpha} = \hat{\psi}_{s\alpha} - L_s i_{s\alpha} \\ \hat{\psi}_{m\beta} = \hat{\psi}_{s\beta} - L_s i_{s\beta} \end{cases} \tag{33}$$

The magnitude of the estimated magnetizing flux can be obtained based in Eq. (33):

$$\hat{\psi}_m = \sqrt{\hat{\psi}_{s\alpha}^2 + \hat{\psi}_{s\beta}^2} \tag{34}$$

In this work, the definition of the magnetizing current magnitude I_m which was presented in [29,30] is taken into account, it is a function of the magnetizing flux, it is expressed a follows:

$$\hat{I}_m = \frac{\hat{\psi}_m}{L_m}\left(a + (1-a)\left(\hat{\psi}_m\, \psi_{mN}\right)^{1-b}\right) \tag{35}$$

The coefficients a and b are the magnetizing curve parameters, their values are the ones used in [29,30], which are $a = 0.9$ and $b = 7$. The rating magnetizing flux ψ_{mN} and the rating magnetizing inductance L_m of the used machine are known initially or can be

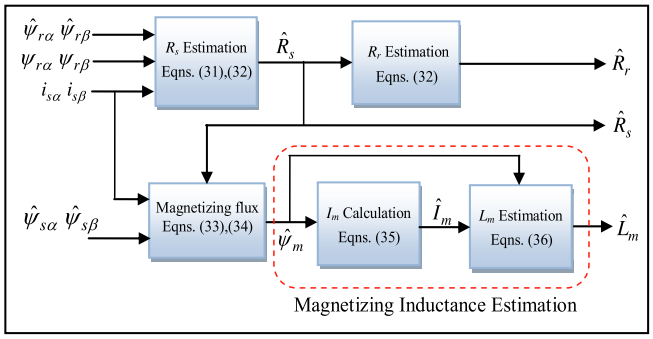

Fig. 7. The basic scheme of the estimation of the motor parameters.

determined experimentally. Since the magnetizing current and the magnetizing flux are estimated, then the magnetizing inductance L_m can be estimated as follows:

$$\hat{L}_m = \frac{\hat{\psi}_m}{\hat{I}_m} \tag{36}$$

The global scheme of the estimation of the studied motor parameters is shown in Fig. 7.

6. Simulation results

For the validation and the evaluation of the advantages of the proposed backstepping control technique presented in this paper for ensuring the control of the dual two-level inverter supplying a FPIM-OESW. Several simulations have been performed at different operation conditions, such as the start-up, the load application, the load variation, the motor parameters change, the high and low speeds and the inversion of the rotation direction. Whereas, the estimation of the rotor speed, the load torque and the motor parameters such as the rotor resistance, the stator resistance and the magnetizing inductance, have been used. The block diagram of the overall control system is shown in Fig. 8. As it has been clearly explained, the proposed backstepping control presented in this paper is based on the MRAS technique and it is combined with the SVPWM to improve the control performances of the overall presented topology of the FPIM and the dual two-level inverter. The electrical and mechanical parameters of the motor are presented in Table 1. Here, the constant reference value of the used rotor flux is set to 0.7 *Wb*.

6.1. First test

The first test has been performed to check the effectiveness and the performance of the used speed sensorless scheme with the estimation of the load torque and the motor parameter. Where, the measured rotor speed is replaced by the one obtained by estimation. In this test, the used reference speed consists of two phases; the first phase varies linearly from zero to the value of the steady state (100 rad/sec) which is reached in 0.5 s. Whereas, the second phase it presents the steady state speed which is constant as shown in Fig. 9. The rotor real speed, the rotor estimated speed and the reference speed of the studied motor starting from the start up instant to 2.5 s are shown in the same figure. It is clear that the proposed speed estimator allows ensuring an accurate tracking of the real speed of the motor, with small response time compared to the simulation results presented in [47,48,51]. A zoom is taken from Fig. 9 around the instant of 0.5 s, shows the precise tracking, especially along the overshoot (0.01 rad/sec) referred to the reference steady state speed. Furthermore, Fig. 10 shows the speed estimation error, which presents the instantaneous difference between the rotor real speed and the rotor estimated speed. Where, this error is nearly equal to 0.005 rad/sec during the transient state of the start-up that is required to reach the reference speed. It is obvious that this estimation error rejoins approximately the zero when the steady state of the motor is

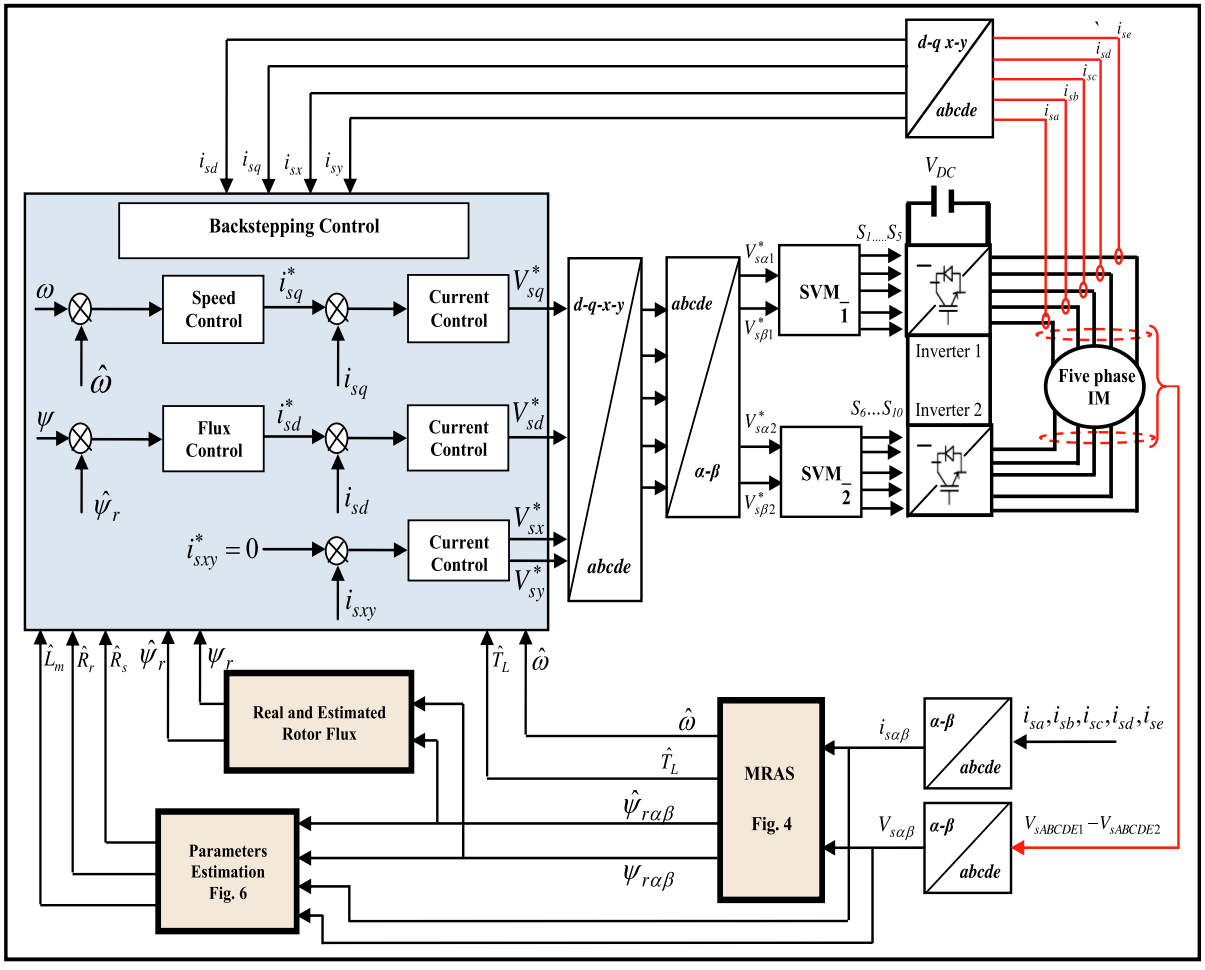

Fig. 8. The basic scheme for the SVM-Backstepping sensorless control of FPIM-OESW based on model reference adaptive system and parameter estimation.

Table 1
The rated data of the FPIM-OESW.

Designation	Notations	Rating values	Unity
Number of poles	n_p	2	/
Stator resistance	R_s	1.2	[Ω]
Rotor resistance	R_r	1.8	[Ω]
Rotor leakage reactance	Ll_r	5.4e-3	[H]
Stator leakage reactance	Ll_s	5.4e-3	[H]
Magnetizing inductance	L_m	0.15	[H]
Moment of inertia	J	0.07	[Kg.m^2]
Friction coefficient	F	0.001	/

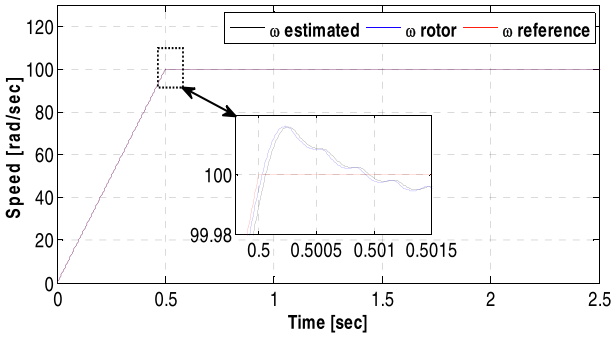

Fig. 9. The reference, real and estimated rotor speed of the studied motor.

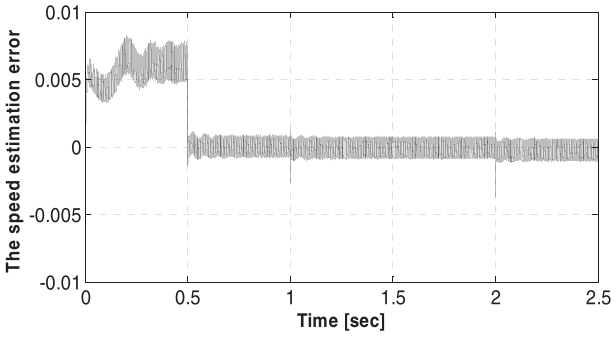

Fig. 10. The speed estimation error.

attained. Indeed, the error tracking is reduced from 5% to 0.5% compared to the error obtain in the work presented in [10,43]at the start up.

Fig. 11 shows the estimated load torque and the reference load torque applied to the shaft of the studied motor, which presents a sequence of step changes. The load torque measurement is expected to be obtained based on the load torque sensor. It is clear that the proposed control allows ensuring accurate load torque estimation with faster response. Indeed, it tracks accurately its reference with a neglected estimation error which equals nearly zero as shown in Fig. 12. The angular rotor position is shown in Fig. 13, it varies between zero and 2π rad. It is clear that it presents a periodic function, however due to the acceleration phenomena during the start-up (between 0 s and 0.5 s) the period decreases following the increase of the rotor speed until it reaches a constant value at around 0.5 s which is corresponding to the steady state reference speed. While Fig. 14 shows the developed electromagnetic torque by the studied motor under the proposed control. It is observed obviously that the developed electromagnetic torque presents high dynamic with fast response and it is equal to the load torque in steady state, where it tracks precisely the imposed step changes of the load torque. The switching ripple is not seen in the developed electromagnetic torque due to the use of the SVPWM which can be consider as an advantage of using this control technique for the considered dual inverter.

The five phase stator currents of the studied FPIM-OESW are shown in Fig. 15. It is clear that the currents behave according to the dynamic behaviour of the motor, which is depending on the load torque change, where sinusoidal waveforms are obtained with reduced harmonic content and their magnitudes change following the developed torque. In the same time the stator five phase current are balanced as it can be seen clearly in the zoom area shown in Fig. 15.

Fig. 16 shows the studied motor direct and quadratic stator currents (i_{sd},i_{sq}) in the synchronous frame. It can be noticed that the direct stator current (i_{sd}) is presenting the image of the rotor flux and it takes nearly constant value and both of them behave in the same way. Whereas, the quadratic stator current (i_{sq}) is proportional to the electromagnetic torque and the i_{sq} is increased to compensate the load torque, when a step load is applied. It is clear that the direct rotor flux represents a fast response in tracking the reference flux (0.7 Wb) as shown in Fig. 17. While the quadratic rotor flux maintains it value nearly equal to zero. This shows that the decoupling between the rotor flux and the torque is achieved and as it is expected, the rotor flux trajectory in the stationary $\alpha - \beta$ frame presents a circular form as shows in Fig. 18. Fig. 19 shows the rotor and stator estimated resistances of the studied motor, it is obvious from the obtained results that the proposed estimator is able to estimate the real values of the stator and rotor resistances accurately within a time less than 0.01 s, even if the load torque is increased. It can be said that this proposed estimator is not affected by the increase of the load torque and it is more faster compared to the previous works presented in [18,23,32,50,52–55]. On the other side, the real and the estimated magnetizing inductance are shown in Fig. 20. It can be seen clearly, that the estimated L_m follows closely the real value. We can also note that we have almost achieved the same simulation results presented in [31]with less complex algorithm.

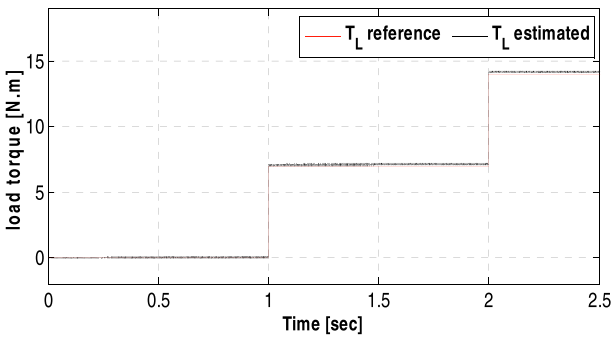

Fig. 11. The reference load torque and the estimated load torque.

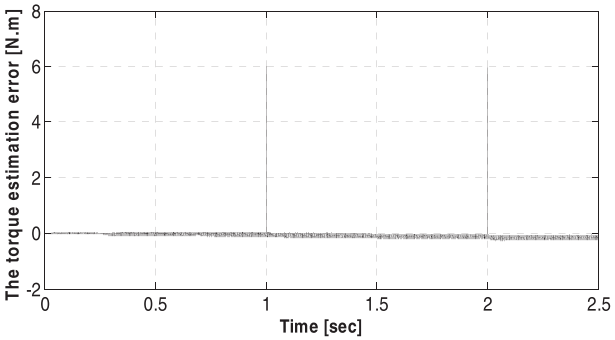

Fig. 12. The load torque estimation error.

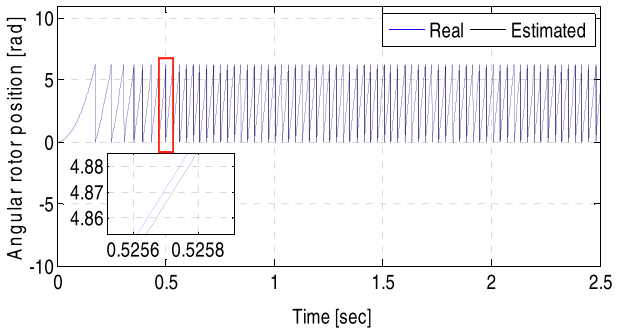

Fig. 13. The real and estimated angular rotor position.

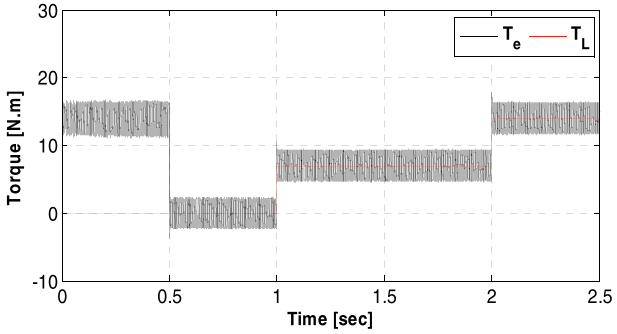

Fig. 14. The motor electromagnetic developed torque and the load torque.

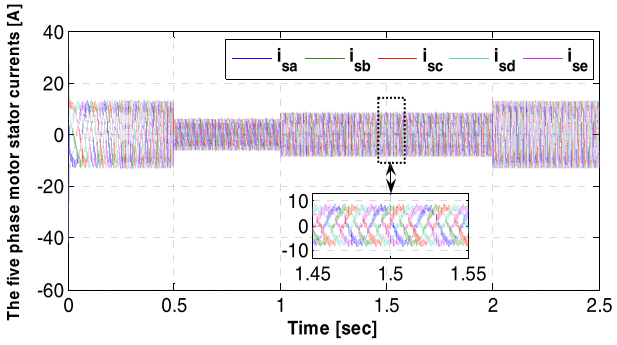

Fig. 15. The FPIM stator currents.

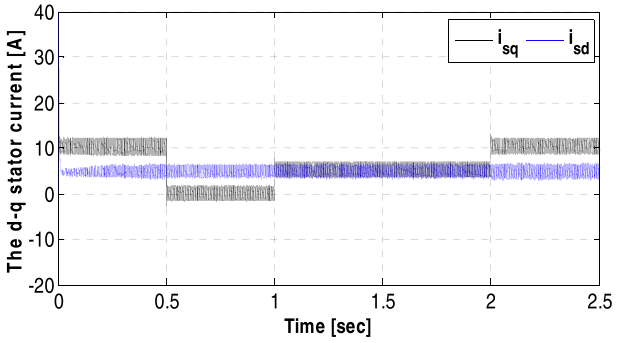

Fig. 16. The d-q stator currents.

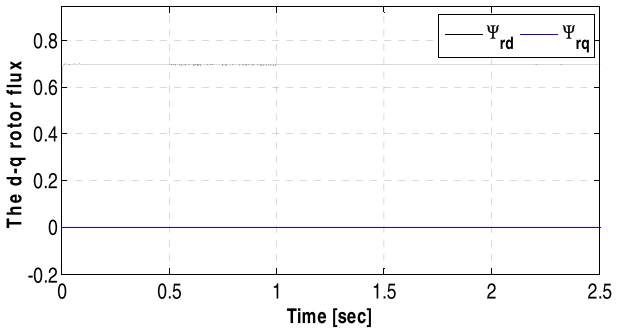

Fig. 17. The d-q rotor flux.

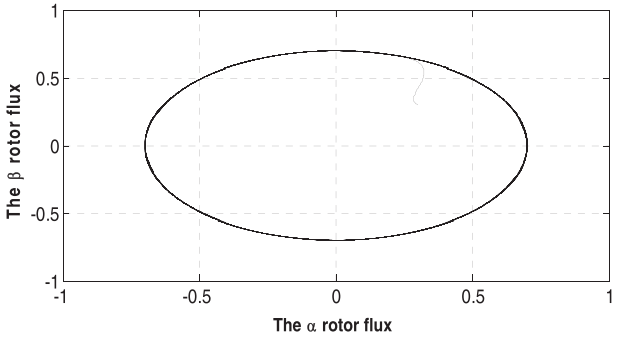

Fig. 18. The rotor flux trajectory in α-β frame.

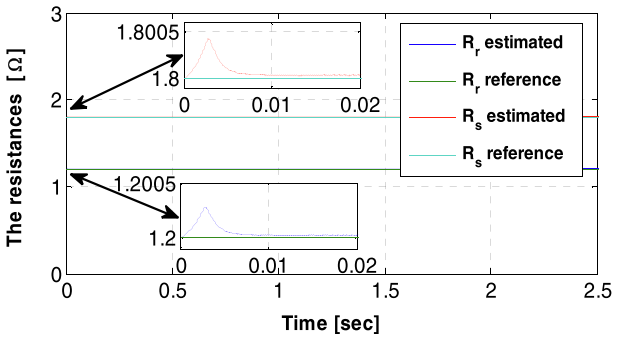

Fig. 19. The reference and estimated resistances of the rotor and stator respectively.

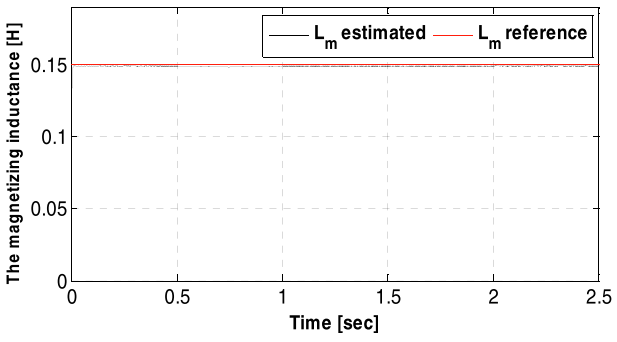

Fig. 20. The reference and estimated magnetizing inductance.

6.2. Second test

In this test, the motor operates under low-speed operation. In order to study the influences of the changes in the motor parameters on the speed estimation, the initial stator resistance of the motor at start-up is $R_s = 1.2\ \Omega$, and after 1 s, R_s is changed from 1.2 to 2.4, meanwhile the rotor resistance R_r is changed from 1.8 to 3.6 during 1 s. It can be seen from Fig. 21 that the estimated values of the stator resistance are not taken into consideration in the used control system during the time between 0 s and 2 s. The parameter estimation system is activated at 2 s as shown in Figs. 21 and 22, where the stator and rotor resistances are estimated by the proposed method. Indeed, the online estimations of the motor parameters, which are proposed to be added to the MRAS estimator, are designed for the enhancement of the low-speed operation dynamics behavior. For this purpose, a simulation test was performed for the motor running at low speed of 2 rad/sec without load torque. It can be seen in Figs. 21 and 22 that the estimated resistances R_s and R_r follow very closely the real values with negligible error. Also, it is observed that the change in stator resistance has no effect on rotor resistance estimation performance.

Fig. 23 shows the rotor reference speed, the rotor estimated speed and the rotor real speed. It can be said that the rotor real speed and the rotor estimated speed converge to the reference speed rapidly. While the rotor estimated speed tracks in an accurate manner the rotor real speed even at a low speed (2 rad/sec) where the tracking estimation error is reduced from 6% to 0.3% compared to the work presented in [16,53,56]. This result proves the high dynamic of the used MRAS estimator in ensuring advantageous stable operation mode of the studied motor at low speeds in comparison with the classical and conventional controllers. The error results between the rotor real speed and the rotor-estimated speed reflects the accuracy quality of the used speed estimator as shown in Fig. 24. Furthermore, based on the obtained results, it can be said that the proposed backstepping control based on MRAS is very sensitive to the variation of the R_s and R_r. Indeed, incorrect values of the resistances can affect remarkably the accuracy of the speed estimation, which means that an increased estimation error between the rotor real speed and the rotor estimated speed makes the MRAS performance poor. In order to avoid this, the activation of the stator and rotor resistance estimators respectively at t = 2 s is performed, consequently a considerable minimization of the estimation error of the speed is obtained as shown clearly in Fig. 24.

6.3. Third test

In order to evaluate and to check the robustness of the used estimator which is proposed in this work, it is important to check the influence of the motor parameters change on the dynamic of the estimator. Therefore, a reverse speed tests without load has been performed following the reference speed, which varies in three steps, from zero to 100 rad/sec, from 100 rad/sec to −100 rad/sec and from −100 rad/sec to zero as shown in Fig. 25.

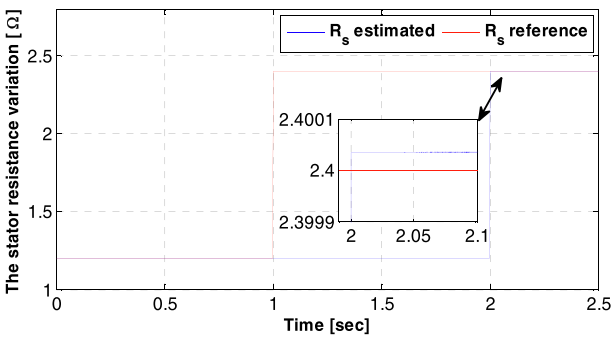

Fig. 21. The reference and estimated stator resistance variations.

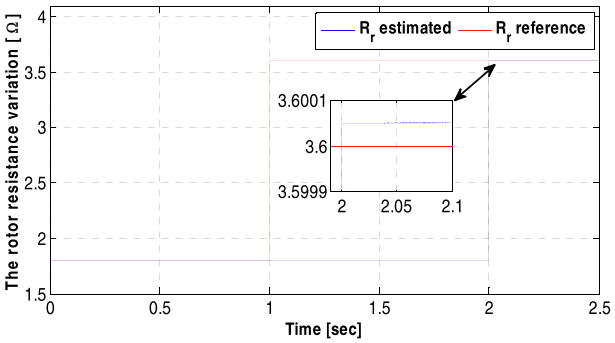

Fig. 22. The reference and estimated rotor resistance variations.

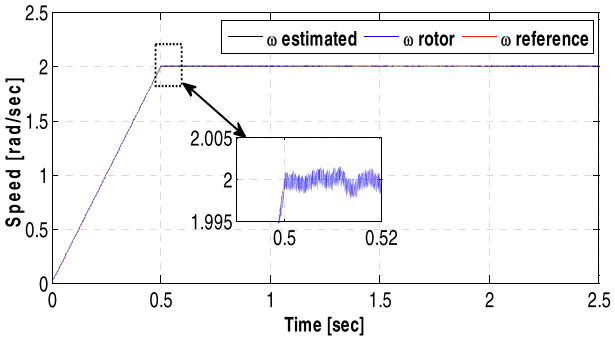

Fig. 23. The real, reference and estimated speed responses.

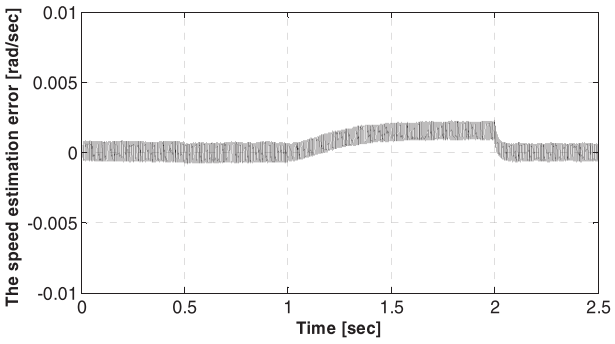

Fig. 24. The speed estimation error.

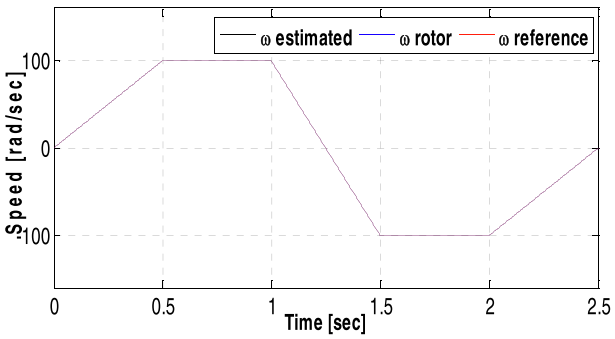

Fig. 25. The rotor speed and the rotor estimated speed variations.

The obtained results shown in Fig. 25 prove clearly that the used estimator allows obtaining a rotor estimated speed which matches perfectly the rotor real speed with improved performance following the various speed variations presented in this test. Furthermore, the good estimation performance of the angular rotor position is ensured as shown in Fig. 26. Indeed, the obtained simulation results of the motor parameter estimation are shown in Fig. 27, where the two estimated resistances reach the real values in a very short time less than 0.003 s and the estimated motor parameters follow the real values during all changes in the reference speed with negligible estimation error, which proves the high-speed response and the accuracy of the proposed estimator.

Finally, based on the obtained results following the three previous tests of the application of proposed backstepping control technique on FPIM-OESW, which is based on the MRAS combined with the SVPWM. It can be said that the proposed backstepping is able to ensure the tracking of the speed reference within a large range with enhanced performance under different speed constraints such as the speed reference variation, the speed reference inversion, the low speed and the load disturbances. Furthermore, the obtained results confirm that the parameter estimation algorithm used in the proposed control is robust under the variation of the studied motor parameters during operating state such as the rotor resistance, the stator resistance and the magnetizing inductance, due to the accurate parameter estimation, where the FPIM-OESW does not loose stability under different operation conditions. In the same time, it is proved that the proposed control technique is also robust to the speed variations and it is not affected by the speed changes and the direction inversion as shown clearly in Fig. 27. These main outstanding features resulting from the application of the proposed backstepping control technique on the FPIM-OESW will permit to such motor to be used in several indusial applications, where the main problems, which can be faced practically, are overcome. Especially, the motor operation interruption due to power supply faults, the difficulties in operating at low and very low speed mainly in high power, more maintenance of the sensors, the appearance of the impact of the common mode voltage and the short lifespan of motor bearings. Indeed, the present study presented in this paper benefits from the main advantage of the five-phase induction machine, the open-end stator windings and the applications of the proposed control technique, which is applied for the first time with the studied topology of FPIM-OESW, where the main aim is to improve the FPIM performances in industrial applications.

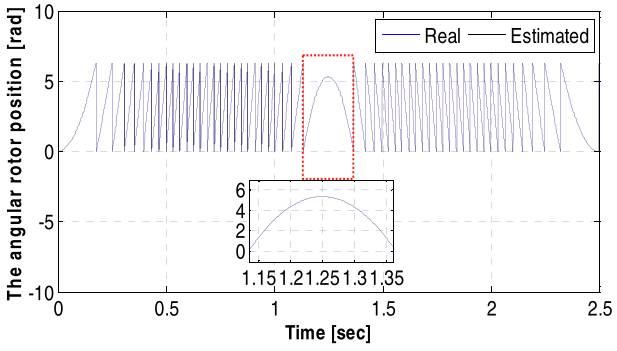

Fig. 26. The rotor and the estimated angular rotor position.

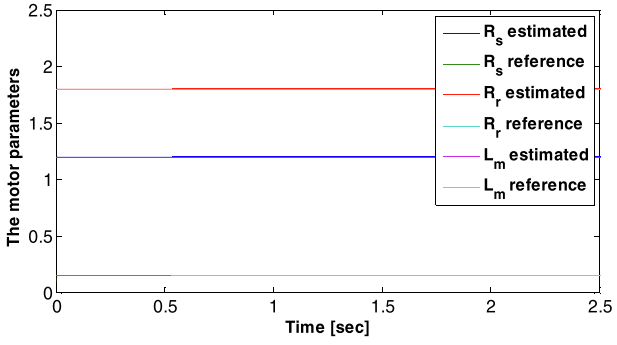

Fig. 27. The resistances of the rotor and stator and the magnetizing inductance.

The proposed technique is based mainly on the measured stator voltage and current, which ensures more simplification of the proposed technique, so that the necessary computing costs can be the minimized as much as possible. On the same time, the proposed technique is different from the previous techniques published in [21–23,27,28,55], where mostly of these techniques suffer from the common problem of complexity, computational intensiveness. Instead, the proposed method is very simple and the process of the rotor speed and the stator resistance estimators operate in parallel rather than in sequential manner. Thus, it can be said that the overall control concept proposed in this paper does not involve a further computational cost and it can be implemented easily in a low-cost microcontroller.

7. Conclusions

In this work, a new control technique based on the backstepping control technique, which is combined with the SVPWM is proposed for the control of a FPIM-OESW topology. Where, the Model Reference Adaptive System concept is used for the estimation of the load torque, the rotor flux and the rotor speed. Furthermore, a high sensitive estimator of the parameters of the studied motor under operation state, such as the rotor resistance, the stator resistance and the magnetizing inductance, is proposed in this work. Indeed, the presented control with the proposed estimators have been tested via simulation under different operation conditions of the studied motor, especially under conditions of load variation, speed variation, rotation inversion, low speed and motor parameter changes. The obtained results demonstrate that the proposed algorithm has a powerful approach to track the variation of the parameters of the studied motor compared to the previous works. The advantage of this algorithm lies in its robustness towards the speed and load torque variations, and it can guarantee a minimal response time with a lowest estimation error.

Based on the obtained results, it can be said that the proposed control technique based on the proposed estimator presents a very competitive and promising solution for the control of the multi-phase machines, especially for the presented topology of OESW. On the other side, this proposed control technique is an original application where it is applied in this work for the first time for the present studied motor topology. It can be said that the proposed control can be used effectively to overcome the main problems faced in controlling the multi-phase machines, especially in high power industrial applications, where the maintenance is difficult and the fault tolerant is required to avoid the motor operating mode interruption within a wide range of speed variation. It can be concluded that the obtained results have proved the improvement of the control performance, the minimization of the computational complexity and the outstanding efficacy of the proposed estimators following different severe operating scenarios.

References

[1] J.M. Apsley, S. Williamson, A.C. Smith, M. Barnes, Induction motor performance as a function of phase number, Proc. Electric Power Appl. 153 (6) (2006) 898–904.

[2] E. Levi, Multiphase electric machines for variable-speed applications, IEEE Trans. Ind. Electron. 55 (5) (2008) 1893–1909.
[3] W. Cao, B.C. Mecrow, G.J. Atkinson, J.W. Bennett, Overview of electric motor technologies used for more electric aircraft (MEA), IEEE Trans. Ind. Electron. 59 (9) (2012) 3523–3531.
[4] S. Kamel, S. Mark, A modelling and simulation of a sensorless control of five-phase PMSM drives using multi-dimension space vector modulation, Telkomnika 14 (4) (2016) 1269–1283.
[5] E. Hamdi, T. Ramzi, I. Atif, M. Mohamed Faouzi, Adaptive Direct Torque Control using Luenberger-Sliding Mode Observer for Online Stator Resistance Estimation for Five-Phase Induction Motor Drives, Springer Electrical Engineering, 2017, pp. 1–11.
[6] L. de-Lillo, L. Empringham, P.W. Wheeler, S. Khwan, C. Gerada, M.N. Othman, X. Huang, Multiphase power converter drive for fault-tolerant machine development in aerospace applications, IEEE Trans. Ind. Electron. 57 (2) (2010) 575–583.
[7] J. Listwan, K. Pieńkowski, Field-oriented control of five-phase induction motor with open-end stator winding, Archiv. Electr. Eng. 65 (03) (2016) 395–410.
[8] R. Sundram, B.J. Auzani, L. V. R. Logan Raj, A. S. Mohamed and A.K. Kasrul, " Improved performance of DTC for 5-phase induction machine using open-end topology," in: Energy Conversion (CENCON), IEEE Conference on. Johor Bahru, Malaysia, Dec. 2014.
[9] H. Ziane, J.M. Retif, T. Rekioua, Fixed-switching-frequency DTC control for PM synchronous machine with minimum torque ripples, Can. J. Electr. Comput. Eng. 33 (2008) 183–189.
[10] F. Farhani, C.B. Regaya, A. Zaafouri, A. Chaari, Real time PI-backstepping induction machine drive with efficiency optimization, ISA Trans. 70 (2017) 348–356.
[11] Y. Zhonggang, L. Guoyin, Z. Yanqing, L. Jing, S. Xiangdong, Z. Yanru, A speed and flux observer of induction motor based on extended kalman filter and markov chain, IEEE Trans. Power Electron. 32 (9) (2017) 7096–7117.
[12] Y.D. Yoon, S.K. Sul, Sensorless control for induction machines based on square-wave voltage injection, IEEE Trans. Power Electron. 29 (7) (2014) 3637–3645.
[13] A. Bennassar, A. Abbou, M. Akherraz, M. Barara, Sensorless backstepping control using an adaptive Luenberger observer with three levels NPC inverter, Int. J. Comput. Electr. Autom. Control Inf. Eng. 7 (8) (2013) 1171–1177.
[14] C. Lascu, I. Boldea, F. Blaabjerg, Direct torque control of sensorless induction motor drives: a sliding-mode approach, IEEE Trans. Ind. Appl. 40 (2) (2004) 582–590.
[15] Y.D. Landau, Adaptive control: the model reference approach, IEEE Trans. Syst. Man Cybern. SMC-14 (1) (1984) 169–170.
[16] A. Pal, S. Das, A.K. Chattopadhyay, An improved rotor flux space vector based MRAS for field-oriented control of induction motor drives, IEEE Trans. Power Electron. 33 (6) (2018) 5131–5141.
[17] A. Khlaief, M. Boussak, A. Châari, A MRAS-based stator resistance and speed estimation for sensorless vector controlled IPMSM drive, Electr. Power Syst. Res. 108 (2014) 1–15.
[18] C.B. Regaya, F. Farhani, A. Zaafouri, A. Chaari, A novel adaptive control method for induction motor based on Backstepping approach using dSpace DS 1104 control board, Mech. Syst. Sig. Process. 100 (2018) 466–481.
[19] G. Kenne, J.D.N. Nguimfack, R.F. Kuate, B.H. Fotsin, An online simplified nonlinear controller for transient stabilization enhancement of DFIG in multi-machine power systems, IEEE Trans. Autom. Control 60 (9) (2015) 2464–2469.
[20] M. Barut, R. Demir, E. Zerdali, R. Inan, Real-time implementation of bi input-extended Kalman filter-based estimator for speed-sensorless control of induction motors, IEEE Trans. Ind. Electron. 59 (11) (2012) 4197–4206.
[21] C.B. Regaya, F. Farhani, A. Zaafouri, A. Chaari, Comparison between two method for adjusting the rotor resistance, Int. Rev. Modell. Simul. 5 (2) (2012) 938–945.
[22] J. Mabrouk, J. Kamel, K. Yassine, B. Mohamed, A Luenberger state observer for simultaneous estimation of speed and rotor resistance in sensorless indirect stator flux orientation control of induction motor drive, Int. J. Comput. Sci. 8 (3) (2011) 116–125.
[23] F. Mapelli, D. Tarsitano, F. Cheli, MRAS rotor resistance estimators for EV vector controlled induction motor traction drive: analysis and experimental results, Electr. Power Syst. Res. 146 (2017) 298–307.
[24] E.D. Mitronikas, A.N. Safacas, E.C. Tatakis, A new stator resistance tuning method for stator-flux-oriented vector-controlled induction motor drive, IEEE Trans. Ind. Electron. 48 (6) (2001) 1148–1157.
[25] H. Kubota, K. Matsuse, "Speed sensorless field oriented control of induction machines using flux observer, in: IEEE Ind. Elect., Contand Instr, IECON '94, Bologna, Italy, Aug. 2002.
[26] L. Umanand, S.R. Bhat, Online estimation of stator resistance of an induction motor for speed control applications, Proc. Inst. Electr. Eng. Electr. Power Appl. 142 (2) (1995) 97–103.
[27] R. Marino, S. Peresada, P. Tomei, On-line stator and rotor resistance estimation for induction motors, IEEE Trans. Control. System. Technol. 8 (2000) 570–579.
[28] G. Guidi, H. Umida, A novel stator resistance estimation method for speed-sensorless induction motor drives, IEEE Trans. Ind. Appl. 36 (2000) 1619–1627.
[29] T. Orlowska-Kowalska, G. Tarchala, M. Dybkowski, Sliding-mode direct torque control and sliding-mode observer with a magnetizing reactance estimator for the field-weakening of the induction motor drive, Math. Comput. Simul. 98 (2014) 31–45.
[30] S.Z. Mohamed, M.K. Mahmoud, S.S. Shokry, A.Y. Hussain, Wide-speed-range estimation with online parameter identification schemes of sensorless induction motor drives, IEEE Trans. Ind. Electron. 56 (5) (2009) 1699–1707.
[31] S. Yang, D. Ding, X. Li, Z. Xie, X. Zhang, L. Chang, A novel online parameter estimation method for indirect field oriented induction motor drives, IEEE Trans. Energy Convers. 32 (4) (2017) 1562–1573.
[32] H. Echeikha, R. Trabelsia, A. Iqbal, M.F. Mimouni, Real time implementation of indirect rotor flux oriented control of a five-phase induction motor with novel rotor resistance adaption using sliding mode observer, J. Franklin Inst. 355 (5) (2018) 2112–2141.
[33] Y.A. Zorgania, Y. Koubaa, M. Boussak, MRAS state estimator for speed sensorless ISFOC induction motor drives with Luenberger load torque estimation, ISA Trans. 61 (2016) 308–317.
[34] M. Morawiec, Dynamic variables limitation for backstepping control of induction machine and voltage source converter, Archiv. Electr. Eng. 61 (3) (2012) 389–410.
[35] M.S. Alam, M. Rizwan Khan, Stability analysis of a five-phase induction motor drive using variable frequency technique, Universal J. Electr. Electron. Eng. 4 (5) (2016) 120–128.
[36] S. Kiran Aher, A.G. Thosar, Modeling and simulation of five phase induction motor using MATLAB/simulink, Int. J. Eng. Res. Appl. 6 (5) (2016) 1–8.
[37] K.B. Subodh, K.J. Kiran, Five-phase induction motor DTC-SVM scheme with PI controller and ANN controller, Procedia Technol. 25 (2016) 816–823.
[38] H. Echeikha, R. Trabelsib, A. Iqbal, N. Bianchiabc, M.F. Mimouni, Non-linear backstepping control of five-phase IM drive at low speed conditions–experimental implementation, ISA Trans. 65 (2016) 244–253.
[39] S.A. Ayman, S. Ahmed, Performance evaluation of a five-phasemodular winding induction machine, IEEE Trans. Ind. Electron. 59 (6) (2012) 2654–2669.
[40] C. Kalaivani, P. Sanjeevikumar, K. Rajambal, B. Frede, Modeling of five-phase, self-excited induction generator for wind mill application, Electr. Power Compon. Syst. (2018) 1–11.
[41] M. Jones, I.N. Wahyu Satiawan, A simple multi-level space vector modulation algorithm for five-phase open-end winding drives, Math. Comput. Simul. 90 (2013) 74–85.
[42] T. Mohammed, K. Mohammed, B. Badre, H. Dalila, L. Ahmed, D. Aziz, Speed variable adaptive backstepping control of the doubly-fed induction machine drive, Int. J. Autom. Control 10 (1) (2016) 13–33.
[43] A. Zaafouri, C.B. Regaya, H.B. Azza, A. Châari, DSP-based adaptive backstepping using the tracking errors for high-performance sensorless speed control of induction motor drive, ISA Trans. 60 (2016) 333–347.
[44] H. Echeikh, R. Trabelsi, A. Iqbal, N. Bianchi, M.F. Mimouni, Comparative study between the rotor flux oriented control and non-linear backstepping control of a five-phase induction motor drive – an experimental validation, IET Power Electron. 9 (13) (2016) 2510–2521.
[45] M. Taoussi, M. Karim, B. Bossoufi, D. Hammoumi, A. Lagrioui, Speed backstepping control of the double-fed induction machine drive, J. Theor. Appl. Inf. Technol. 74 (2) (2015) 189–199.
[46] M. Jones, I.N. Satiawan, N. Bodo, E. Levi, A dual five-phase space-vector modulation algorithm based on the decomposition method, IEEE Trans. Ind. Appl. 48 (6) (2012) 2110–2120.
[47] E. Dehghan-Azad, S. Gadoue, D. Atkinson, H. Slater, P. Barrass, F. Blaabjerg, Sensorless control of im based on stator-voltage MRAS for limp-home EV applications, IEEE Trans. Power Electron. 33 (3) (2018) 1911–1921.
[48] M. Mohamed, A. Ahmed, M. Hassan, MRAS-based sensorless speed backstepping control for induction machine, using a flux sliding mode observer, Turkish J. Electr. Eng. Comput. Sci. 23 (1) (2015) 187–200.
[49] V. Vasic, S.N. Vukosavic, E. Levi, A Stator resistance estimation scheme for speed sensorless rotor flux oriented induction motor drives, IEEE Trans. Energy Convers. 18 (4) (2003) 476–483.
[50] S.M.N. Hasan, I. Husain, A Luenberger-sliding mode observer for online parameter estimation and adaptation in high- performance induction motor drives, IEEE Trans. Ind. Appl. 45 (2) (2009) 771–781.
[51] M.R. Khan, A. Iqbal, M. Ahmad, MRAS-based sensorless control of a vector controlled five-phase induction motor drive, Electr. Power Syst. Res. 78 (2008) 1311–1321.
[52] J. Chen, J. Huang, Online decoupled stator and rotor resistances adaptation for speed sensorless induction motor drives by a time-division approach, IEEE Trans. Power Electron. 32 (2017) 4587–4599.
[53] P.L. Roncero-Sánchez, A. García-Cerrada, V. Feliu-Batlle, "Rotor-resistance estimation for induction machines with indirect-field orientation, Control Eng. Pract. 15 (9) (2007) 1119–1133.
[54] A.B. Proca, A. Keyhani, Sliding-mode flux observer with online rotor parameter estimation for induction motors, IEEE Trans. Ind. Electron. 54 (2) (2007) 716–723.
[55] M. Hinkkanen, L. Harnefors, J. Luomi, Reduced-order flux observers with stator-resistance adaptation for speed-sensorless induction motor drives, IEEE Trans. Power Electron. 25 (5) (2010) 1173–1183.
[56] R. Trabelsi, A. Khedher, M. Faouzi, M. Faouzi, An adaptive backstepping observer for on-line rotor resistance adaptation, Int. J. Sci. Tech. Autom. Control Comput. Eng. 4 (1) (2010) 1246–1267.